

# The juvenile myoclonic epilepsy mutant of the calcium channel $\beta_4$ subunit displays normal nuclear targeting in nerve and muscle cells

Solmaz Etemad<sup>†</sup>, Marta Campiglio<sup>†</sup>, Gerald J Obermair, and Bernhard E Flucher\*

Division of Physiology; Department of Physiology and Medical Physics; Medical University Innsbruck; Innsbruck, Austria

<sup>†</sup>These authors contributed equally to this work.; Keywords: *CACNB4*,  $\text{Ca}_v\beta_4$  subunit, voltage-gated  $\text{Ca}^{2+}$  channel, hippocampal neurons, dysgenic myotubes

**Abbreviations:**  $\text{Ca}_v$ , voltage-gated calcium channel; PP2A, protein phosphatases 2A; HP1 $\gamma$ , heterochromatin protein 1 gamma; DIV, days in vitro

Voltage-gated calcium channels regulate gene expression by controlling calcium entry through the plasma membrane and by direct interactions of channel fragments and auxiliary  $\beta$  subunits with promoters and the epigenetic machinery in the nucleus. Mutations of the calcium channel  $\beta_4$  subunit gene (*CACNB4*) cause juvenile myoclonic epilepsy in humans and ataxia and epileptic seizures in mice. Recently a model has been proposed according to which failed nuclear translocation of the truncated  $\beta_4$  subunit R482X mutation resulted in altered transcriptional regulation and consequently in neurological disease. Here we examined the nuclear targeting properties of the truncated  $\beta_{4b(1-481)}$  subunit in tsA-201 cells, skeletal myotubes, and in hippocampal neurons. Contrary to expectation, nuclear targeting of  $\beta_{4b(1-481)}$  was not reduced compared with full-length  $\beta_{4b}$  in any one of the three cell systems. These findings oppose an essential role of the  $\beta_4$  distal C-terminus in nuclear targeting and challenge the idea that the nuclear function of calcium channel  $\beta_4$  subunits is critically involved in the etiology of epilepsy and ataxia in patients and mouse models with mutations in the *CACNB4* gene.

## Introduction

The auxiliary  $\beta$  subunits of voltage-gated calcium channels promote membrane expression and modulate the gating properties of  $\text{Ca}_v1$  and  $\text{Ca}_v2$  calcium channels. In humans four genes encode  $\text{Ca}_v\beta$  subunits and abundant alternative splicing further increases the molecular heterogeneity of the  $\beta$  subunit family. Co-expression studies demonstrated that all  $\beta$  isoforms promote membrane expression of any  $\text{Ca}_v1$  and  $\text{Ca}_v2$  channel isoform and modulate their gating properties in a similar way.<sup>1</sup>

These highly promiscuous isoform interactions generate a considerable functional redundancy of  $\beta$  subunits. Consequently, loss-of-function mutations and knockouts of  $\beta$  subunit genes caused a disease phenotype primarily in those tissues that express exclusively the mutated  $\beta$  isoform.<sup>2-5</sup> In contrast, in brain, where all four  $\beta$  subunit genes are expressed, phenotypes were mild or non-existent, most likely because the channel function of the mutated  $\beta$  isoform was compensated by other  $\beta$  isoforms.<sup>6-8</sup> However, there is one notable exception: spontaneous mutations of the  $\beta_4$  subunit lead to idiopathic generalized epilepsy and episodic ataxia in humans and in mice.<sup>9,10</sup> In cerebellum  $\beta_4$  and  $\alpha_2\delta-2$  are the major subunit partners of the P/Q-type ( $\text{Ca}_v2.1$ ) calcium channel. Interestingly, mutations of all three subunit isoforms ( $\text{Ca}_v2.1$ ,  $\alpha_2\delta-2$  and  $\beta_4$ ) result in an epileptic and ataxic

phenotype.<sup>9,11,12</sup> This is consistent with the notion that a deficiency of the P/Q-type channel function causes the neurological disease in  $\beta_4$  mutants.

Recently, we and others discovered that specific  $\beta_4$  subunit isoforms can also accumulate in the nucleus.<sup>13-16</sup> This unexpected finding suggested a role of  $\beta_4$  in channel-independent cell functions. Furthermore, in excitable cells nuclear export of  $\beta_{4b}$  was shown to be activity-dependent. We demonstrated that in skeletal myotubes and in hippocampal neurons  $\beta_{4b}$  accumulated in the nuclei during early development and in electrically quiescent cells and that it was rapidly exported in response to depolarization.<sup>15,17</sup> Because a truncated  $\beta_{4c}$  isoform has previously been shown to interact with the nuclear protein HP1 $\gamma$ , a possible function in gene regulation has been suggested.<sup>14,18</sup> This calcium channel-independent nuclear function provided an alternative explanation for the etiology of the severe neurological phenotype of  $\beta_4$  mutations. If mutated  $\beta_4$  subunits differ from wildtype  $\beta_4$  isoforms with regard to their nuclear targeting properties or their ability to interact with nuclear proteins, then the loss of the nuclear function of  $\beta_4$  may cause the neurological deficits observed in human patients and in mouse models with mutations in the  $\beta_4$  gene. Consistent with this idea, Tadmouri et al.<sup>16</sup> reported that the ataxia mutation R482X resulted in a C-terminally truncated  $\beta_4$  protein, which failed to be targeted into the nucleus and

\*Correspondence to: Bernhard E Flucher; Email: bernhard.e.flucher@i-med.ac.at  
Submitted: 03/12/2014; Revised: 05/22/2014; Accepted: 05/22/2014  
<http://dx.doi.org/10.4161/chan.29322>

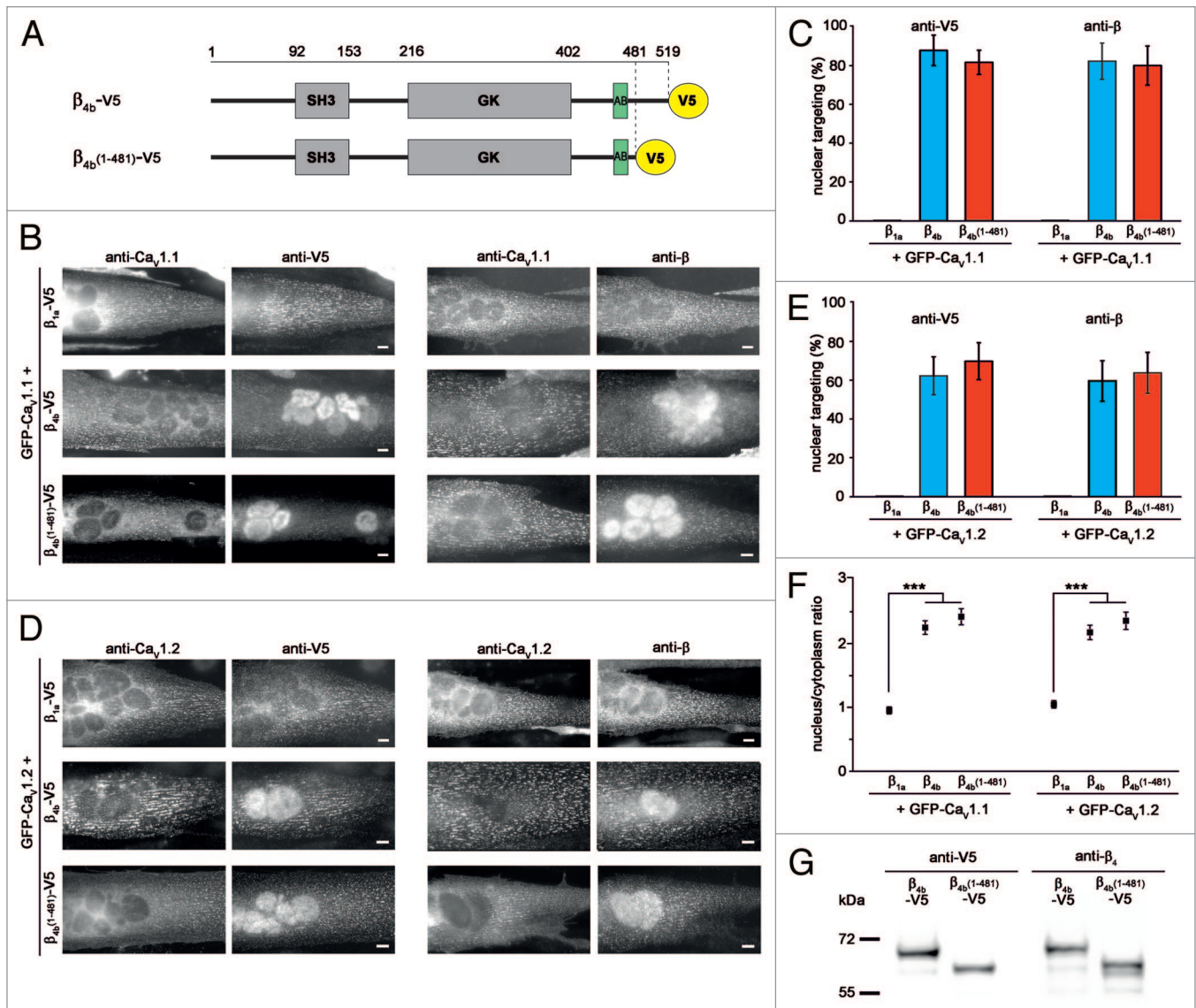


**Figure 1.** Nuclear targeting of V5-tagged wildtype and mutant  $\beta_{4b}$  subunits in dysgenic myotubes. **(A)** Domain structure of the full-length  $\beta_{4b}$ -V5 and truncated  $\beta_{4b(1-481)}$ -V5 subunits. Colored symbols indicate positions of antibody epitopes and numbers above indicate amino acid positions at domain borders and truncation site. **(B)** Representative double-immunofluorescence images of myotubes transfected with  $\beta_{1a}$ -V5,  $\beta_{4b}$ -V5, and  $\beta_{4b(1-481)}$ -V5 together with GFP- $\text{Ca}_v1.1$ , labeled with anti-GFP and anti-V5 (left) or anti- $\beta$  (right). **(C)** Fraction of myotubes showing nuclear targeting, transfected and labeled as in **(B)** ( $\beta_{1a}$ ,  $\beta_{4b}$ ,  $\beta_{4b(1-481)}$ : N = 3; anti-V5 n = 120, anti- $\beta$  n = 150). **(D)** Double-immunofluorescence images of myotubes transfected with  $\beta_{1a}$ -V5,  $\beta_{4b}$ -V5, and  $\beta_{4b(1-481)}$ -V5 together with GFP- $\text{Ca}_v1.2$ , labeled with anti-GFP and anti-V5 (left) or anti- $\beta$  (right). **(E)** Fraction of myotubes showing nuclear targeting, transfected and labeled as in **(D)** ( $\beta_{1a}$ ,  $\beta_{4b}$ ,  $\beta_{4b(1-481)}$ : N = 4; anti-V5 n = 150, anti- $\beta$  n = 210). Note that all  $\beta$  subunits co-cluster with the  $\text{Ca}_v1$  channels throughout the myotubes, but only the two  $\beta_{4b}$  subunit constructs accumulate in the nuclei. **(F)** Nucleus/cytoplasm ratios of myotubes labeled with anti-V5. ANOVA for  $\beta$  subunits co-expressed with GFP- $\text{Ca}_v1.1$  ( $\beta_{4b}$ ,  $\beta_{4b(1-481)}$ : N = 3, n = 60;  $\beta_{1a}$ : N = 1, n = 20):  $F_{(2,137)} = 23.8$   $P = 1.3 \times 10^{-9}$ ; ANOVA for  $\beta$  subunits co-expressed with GFP- $\text{Ca}_v1.2$  ( $\beta_{4b}$ ,  $\beta_{4b(1-481)}$ : N = 4, n = 80;  $\beta_{1a}$ : N = 1, n = 20):  $F_{(2,177)} = 1.7$ ;  $P = 2.6 \times 10^{-5}$  (P values in the figure are for post-hoc analysis; \*\*\* $P < 0.001$ ). Scale bars, 10  $\mu\text{m}$ . **(G)** western blot analysis of  $\beta_{4b}$ -V5 and  $\beta_{4b(1-481)}$ -V5 in dysgenic myotubes with anti-V5 and anti- $\beta_4$  antibodies reveals that both proteins are expressed at similar levels and at the expected size, 15 s exposure (n = 4).

consequently did not interact with the regulatory protein complex shown to repress tyrosine hydroxylase expression. Moreover, in a follow-up study the same group showed that heterologous expression of the full-length and truncated  $\beta_{4b}$  isoform in HEK293 cells resulted in differential gene expression.<sup>19</sup>

Because we recently could demonstrate that in neurons only those  $\beta_4$  splice variants capable of targeting to the nucleus also regulated genes,<sup>17</sup> we set out to examine the nuclear targeting

function of the truncated ataxia mutant in nerve and muscle cells. Unexpectedly, however, wildtype and truncated  $\beta_{4b}$  variants displayed identical nuclear targeting properties. Thus, the data presented here contradict the previous report and challenge the idea that differences in transcriptional regulation due to differential nuclear targeting of the wildtype and mutated  $\beta_{4b}$  subunits may account for the neurological phenotypes in humans and mice with mutations in the *CACNB4* gene.

**Table 1. Nuclear Targeting**

Dysgenic myotubes									
	$\beta_{1a}$ -V5		$\beta_{4b}$ -V5		$\beta_{4b(1-481)}$ -V5		t test		
	anti-V5	anti- $\beta_1$	anti-V5	anti- $\beta_4$	anti-V5	anti- $\beta_4$	anti-V5	anti- $\beta_4$	
+ GFP- $\text{Ca}_v1.1$	0,0%	0,0%	87,2 ± 7,8%	81,7 ± 9,3%	81,1 ± 6,2%	79,4 ± 10,0%	$P = 0.57$	$P = 0.88$	
+ GFP- $\text{Ca}_v1.2$	0,0%	0,0%	62,1 ± 9,8%	59,6 ± 10,4%	69,6 ± 9,5%	63,8 ± 10,5%	$P = 0.89$	$P = 0.79$	
	$\beta_{4b}$				$\beta_{4b(1-481)}$		t test		
	anti- $\beta_4$				anti- $\beta_4$		anti- $\beta_4$		
+ GFP- $\text{Ca}_v1.1$	90,6 ± 1,1%				90,8 ± 2,1%		$P = 0.91$		
+ GFP- $\text{Ca}_v1.2$	74,6 ± 3,7%				78,8 ± 2,8%		$P = 0.41$		
tsA-201									
	$\beta_{1a}$ -V5		$\beta_{4b}$ -V5		$\beta_{4b(1-481)}$ -V5		t test		
	anti-V5	anti- $\beta_1$	anti-V5	anti- $\beta_4$	anti-V5	anti- $\beta_4$	anti-V5	anti- $\beta_4$	
w/o	0 ± 0,0%	0 ± 0,0%	98,9 ± 0,6%	98,9 ± 1,1%	99,8 ± 0,7%	94,4 ± 2,2%	$P = 0.79$	$P = 0.15$	
+ GFP- $\text{Ca}_v1.2/\alpha_2\delta-1$	0 ± 0,0%	0 ± 0,0%	60,6 ± 1,1%	64,4 ± 4,8%	65,6 ± 10,1%	63,3 ± 8,4%	$P = 0.65$	$P = 0.91$	

\*t test between  $\beta_{4b}$ -V5 and  $\beta_{4b(1-481)}$ -V5,  $\beta_{1a}$ -V5 is shown as comparison. For n values refer to the legends of **Figure 1** (dysgenic myotubes) and **Figure 3** (tsA-201)

## Results

### Similar incorporation into calcium channel complexes and nuclear targeting of the full-length and truncated $\beta_{4b}$ subunits in skeletal myotubes

In order to analyze the nuclear targeting properties of the wildtype and ataxia mutant of the  $\beta_4$  subunit in muscle and nerve cells, we generated a truncated  $\beta_{4b}$  construct lacking the 39 C-terminal residues ( $\beta_{4b(1-481)}$ )<sup>10,16</sup> (**Fig. 1A**). Both the wildtype  $\beta_{4b}$  and truncated  $\beta_{4b(1-481)}$  were V5-tagged at the C-terminus to enable specific localization of the heterologous  $\beta_4$  subunits in neurons expressing also endogenous  $\beta_4$ . Extensive previous analysis<sup>15,17</sup> demonstrated that the V5-tagged  $\beta_4$  subunits can functionally interact with  $\text{Ca}_v$  channels in the membrane and show normal nuclear targeting properties when expressed in muscle or nerve cells. Western blot analysis of the full-length  $\beta_{4b}$ -V5 and the truncated  $\beta_{4b(1-481)}$ -V5 constructs confirms that the two  $\beta_4$  subunits express as intact proteins of the expected size (**Fig. 1G**).

First we expressed the full-length  $\beta_{4b}$ -V5 and truncated  $\beta_{4b(1-481)}$ -V5 subunits in dysgenic myotubes. These muscle cells lack the endogenous  $\text{Ca}_v1.1$  channel but otherwise express the full complement of calcium signaling proteins, including the auxiliary  $\text{Ca}_v\beta_{1a}$  and  $\alpha_2\delta-1$  subunits and the ryanodine receptor. Therefore transfection with  $\text{Ca}_v\alpha_1$  subunits reconstitutes the calcium channel in dysgenic myotubes and incorporates the heterologous  $\beta$  subunits into the functional excitation-contraction coupling apparatus.<sup>20</sup> Morphologically this is seen as co-clusters of the heterologously expressed  $\text{Ca}_v\alpha_1$  and  $\beta$  subunits in peripheral couplings and developing triads. When the  $\beta$  subunit constructs ( $\beta_{1a}$ -V5,  $\beta_{4b}$ -V5,  $\beta_{4b(1-481)}$ -V5) were co-expressed with the pore-forming subunit GFP- $\text{Ca}_v1.1$  and immunolabeled with antibodies against GFP and the V5 tag or the  $\beta_1$  or  $\beta_4$  proteins, the calcium channel subunits co-clustered

at the cell surface (**Fig. 1B**). Qualitatively, co-clustering of  $\beta_{4b}$ -V5 and  $\text{Ca}_v1.1$  was not different from that of  $\beta_{1a}$ -V5 and  $\text{Ca}_v1.1$ , although quantitatively co-clustering of the native skeletal muscle subunit partners ( $\beta_{1a}$ -V5 and  $\text{Ca}_v1.1$ ) was more robust than that of the heterologous pair ( $\beta_{4b}$ -V5 and  $\text{Ca}_v1.1$ ).<sup>21</sup> Nevertheless, co-clustering with  $\text{Ca}_v1.1$  confirms previous findings showing that  $\beta_{4b}$  can interact with  $\text{Ca}_v1.1$ <sup>15,21</sup> and it further demonstrates that the C-terminal truncation does not perturb the interaction of  $\beta_{4b(1-481)}$ -V5 with the skeletal muscle calcium channel complex. Consistent with previous findings,<sup>22,23</sup> normal incorporation of  $\text{Ca}_v$  subunits in triads and peripheral couplings was not limited to the skeletal muscle  $\text{Ca}_v1.1$  channel. Also co-expression of the  $\beta_{4b}$ -V5 constructs and GFP- $\text{Ca}_v1.2$  resulted in the typical clustered distribution of both channel subunits in dysgenic myotubes (**Fig. 1D**) and the truncated  $\beta_{4b(1-481)}$ -V5 isoform was as efficiently incorporated into the calcium channel complex as the full-length  $\beta_{4b}$ -V5.

In addition to its incorporation into the channel complexes at the membrane  $\beta_{4b}$ -V5 accumulated in the nuclei of the dysgenic myotubes (**Fig. 1B**). As previously shown<sup>15</sup> this nuclear targeting was specific to the  $\beta_{4b}$ -V5 isoform and rarely observed with  $\beta_{1a}$ -V5. Unexpectedly however, the truncated  $\beta_{4b(1-481)}$ -V5 construct also accumulated in the nuclei of the myotubes. Co-clustering with the  $\text{Ca}_v1.1$  channel and the accumulation of both  $\beta_{4b}$ -V5 and  $\beta_{4b(1-481)}$ -V5 in the nuclei was observed with the V5 tag antibody (**Fig. 1B**, left panels) as well as with the  $\beta_4$  antibody (**Fig. 1B**, right panels). The prevalence of nuclear targeting was quantified by assessing the fraction of transfected differentiated myotubes showing nuclear V5 or  $\beta_4$  staining (**Fig. 1C**; **Table 1**). Whereas no myotubes with nuclear targeting of  $\beta_{1a}$ -V5 were observed, the  $\beta_{4b}$ -V5 constructs were targeted into the nuclei of approximately 80% of the myotubes when co-expressed with  $\text{Ca}_v1.1$ , both when stained with the V5 or with the  $\beta_4$  antibody. Most importantly, the truncated  $\beta_{4b(1-481)}$ -V5 was as frequently found in the nuclei

**Table 2.** Nucleus/Cytoplasm ratio

Dysgenic myotubes			
	$\beta_{4b}$ -V5	$\beta_{4b(1-481)}$ -V5	ANOVA*
+ GFP-Ca <sub>v</sub> 1.1	2.25 ± 0.11	2.42 ± 0.13	<i>P</i> < 0.001
+ GFP-Ca <sub>v</sub> 1.2	2.03 ± 0.11	2.17 ± 0.12	<i>P</i> < 0.001
Hippocampal neurons			
	$\beta_{4b}$ -V5	$\beta_{4b(1-481)}$ -V5	<i>t</i> test
DIV1	1.55 ± 0.03	1.42 ± 0.03	<i>P</i> = 0.66
DIV2	1.47 ± 0.02	1.52 ± 0.02	<i>P</i> = 0.21
DIV3	1.36 ± 0.01	1.44 ± 0.01	<i>P</i> = 0.79
DIV5	0.8 ± 0.02	0.75 ± 0.01	<i>P</i> = 0.12
DIV14	0.72 ± 0.01	0.78 ± 0.02	<i>P</i> = 0.84
DIV21	0.81 ± 0.01	0.72 ± 0.01	<i>P</i> = 0.33
DIV21 + TTX	1.54 ± 0.03	1.57 ± 0.03	<i>P</i> = 0.77

\*For ANOVA parameters and *n* values refer to the legends of **Figure 1** (dysgenic myotubes) and **Figure 2** (hippocampal neurons).

as the full-length  $\beta_{4b}$  construct. To determine whether the extent of nuclear targeting differed between full-length  $\beta_{4b}$  and the truncated  $\beta_{4b(1-481)}$ -V5, we analyzed the nucleus to cytoplasm ratio of the anti-V5 labeled constructs (**Fig. 1F**). The nucleus/cytoplasm ratio of the control  $\beta_{1a}$ -V5 staining was near 1, owing to the uniform distribution of  $\beta_{1a}$ -V5 clusters throughout the myotubes. In contrast, the nucleus/cytoplasm ratios of both  $\beta_{4b}$ -V5 constructs were above 2, reflecting their strong nuclear staining. The nucleus/cytoplasm ratio of the truncated  $\beta_{4b(1-481)}$ -V5 was not statistically different from that of the full-length  $\beta_{4b}$ -V5 (**Table 1**).

To examine whether these targeting properties depended on the co-expressed  $\alpha_1$  subunit, the experiments were repeated with  $\beta_{1a}$ -V5,  $\beta_{4b}$ -V5, and  $\beta_{4b(1-481)}$ -V5 co-expressed with the cardiac/neuronal Ca<sub>v</sub>1.2 channel isoform. **Figure 1D** shows that  $\beta_{4b}$ -V5 and  $\beta_{4b(1-481)}$ -V5, but not  $\beta_{1a}$ -V5, were targeted into the nuclei of the myotubes. This was equally seen when labeled with the V5 or with the  $\beta$  antibody. Also counting the frequency of myotubes with nuclear targeting and analyzing the nucleus/cytoplasm ratios failed to detect any significant difference in the nuclear targeting of  $\beta_{4b}$ -V5 and  $\beta_{4b(1-481)}$ -V5 (**Fig. 1E and F; Tables 1 and 2**). Together these results demonstrate that—when co-expressed with L-type calcium channel  $\alpha_1$  subunits in dysgenic myotubes—the truncated ataxia mutant  $\beta_{4b(1-481)}$ -V5 was efficiently targeted into the nuclei of as many cells as the full-length  $\beta_{4b}$ -V5 subunit.

To exclude the possibility that the C-terminal V5 tag affected the nuclear targeting properties of the heterologous  $\beta_{4b}$  subunits, we generated two corresponding  $\beta_{4b}$  constructs ( $\beta_{4b}$  and  $\beta_{4b(1-481)}$ ) without the V5 tag (**Fig. 2A**). When expressed in dysgenic myotubes together with either GFP-Ca<sub>v</sub>1.1 or GFP-Ca<sub>v</sub>1.2 and immunolabeled with the anti- $\beta_4$  antibody, both  $\beta_{4b}$  and  $\beta_{4b(1-481)}$  were observed in co-clusters with the Ca<sub>v</sub>1 subunits, confirming their expected association with the calcium channels in the membrane, and both  $\beta_{4b}$  and  $\beta_{4b(1-481)}$  were concentrated in

the nuclei (**Fig. 2B**). Semiquantitative analysis showed that the untagged  $\beta_{4b}$  subunits were targeted into the nuclei as efficiently as the V5-tagged versions (compare **Figure 2C** with **Figure 1C and E**). Again, there were no statistically significant differences in number of myotubes showing nuclear targeting between the full-length  $\beta_{4b}$  and the truncated  $\beta_{4b(1-481)}$  isoform (**Table 1**). These experiments clearly demonstrate that fusing a V5 antibody-tag to the C-terminus of neither the full-length  $\beta_{4b}$  nor to the truncated C-terminus of  $\beta_{4b(1-481)}$  alters their nuclear targeting properties.

#### Nuclear targeting of the full-length $\beta_{4b}$ -V5 and the truncated $\beta_{4b(1-481)}$ -V5 subunits in cultured hippocampal neurons

Because we did not detect reduced nuclear targeting properties of the truncated  $\beta_{4b(1-481)}$ -V5 subunit in the skeletal myotubes, we decided to directly compare nuclear targeting of  $\beta_{4b}$ -V5 and  $\beta_{4b(1-481)}$ -V5 in cultured hippocampal neurons. These neurons express all  $\beta$  isoforms in pre- and post-synaptic compartments throughout the neurons.<sup>24,25</sup> In addition the  $\beta_{4b}$  isoform is specifically targeted into the nuclei of young (DIV1–4) and electrically silenced differentiated neurons (DIV17).<sup>15,17</sup> Here we transfected hippocampal neurons with  $\beta_{4b}$ -V5 and  $\beta_{4b(1-481)}$ -V5 and immunolabeled them with anti-V5 to specifically detect the recombinant  $\beta_{4b}$ -V5 constructs. Both  $\beta_{4b}$ -V5 subunits were localized in a punctate distribution pattern in the soma and throughout the neuronal processes (**Fig. 3C**), indicative of their incorporation in pre- and postsynaptic calcium channel complexes. In neurons at DIV1, 2, and 3  $\beta_{4b}$ -V5 as well as  $\beta_{4b(1-481)}$ -V5 also labeled the neuronal nuclei, whereas at later developmental stages (DIV5, 14, and 21) the nuclei were devoid of  $\beta_{4b}$  staining (**Fig. 3A**). Measuring the fluorescent staining intensity of the nucleus and cytoplasm of neurons and calculating the nucleus/cytoplasm ratio showed a high ratio during the first three days in culture followed by a rapid decline and continued low nucleus/cytoplasm ratio from DIV5 onward (**Fig. 3B**). Importantly, the nuclear targeting at the early developmental



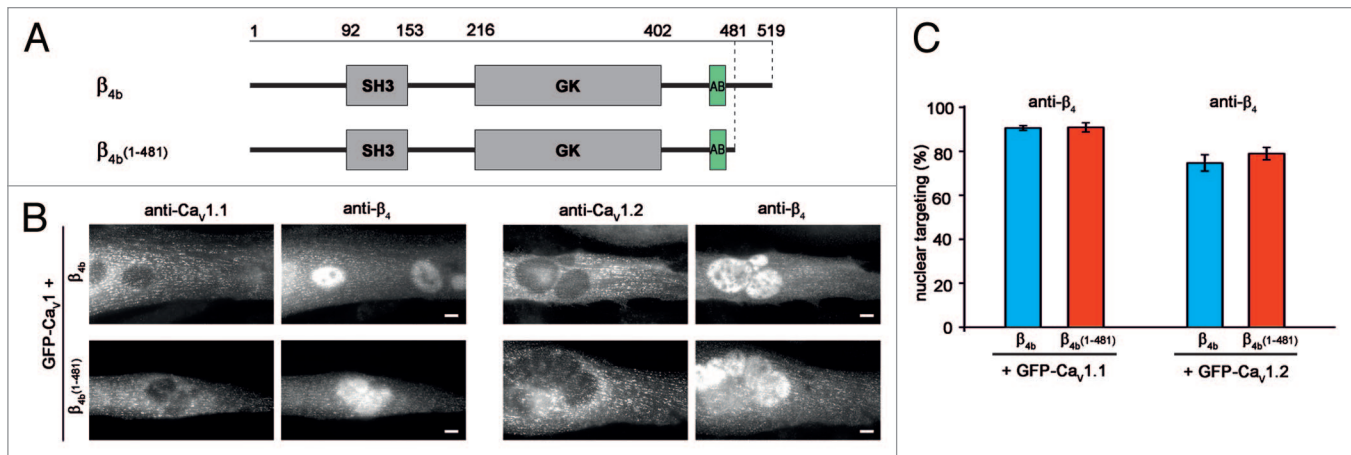


**Figure 2.** Nuclear targeting of untagged wildtype and mutant  $\beta_{4b}$  subunits in dysgenic myotubes. **(A)** Domain structure of the full-length  $\beta_{4b}$  and truncated  $\beta_{4b(1-481)}$  subunits. Colored symbols indicate positions of antibody epitopes and numbers above indicate amino acid positions at domain borders and truncation site. **(B)** Representative double-immunofluorescence images of myotubes transfected with  $\beta_{4b}$  and  $\beta_{4b(1-481)}$  together with GFP- $\text{Ca}_v1.1$  (left) or GFP- $\text{Ca}_v1.2$  (right), labeled with anti-GFP and anti- $\beta_4$ . **(C)** Fraction of myotubes showing nuclear targeting, transfected and labeled as in **(B)** ( $\beta_{4b}$  and  $\beta_{4b(1-481)}$  with GFP- $\text{Ca}_v1.1$ :  $N = 4$   $n = 360$ ; ( $\beta_{4b}$  and  $\beta_{4b(1-481)}$  with GFP- $\text{Ca}_v1.2$ :  $N = 3$   $n = 240$ ).

stage as well as the lack thereof in differentiated neurons was identical for  $\beta_{4b}$ -V5 and  $\beta_{4b(1-481)}$ -V5 (Table 2).

Because previously we detected that nuclear export of  $\beta_{4b}$  in differentiated neurons was activity dependent, we examined whether this was also the case for the truncated  $\beta_{4b(1-481)}$ -V5 subunit. Therefore we blocked spontaneous electric activity in three weeks old (DIV21) hippocampal neurons by overnight incubation with 1  $\mu\text{M}$  TTX just prior to fixation and immunolabeling. As shown in Figure 3A and B, TTX treatment restored nuclear targeting of both  $\beta_{4b}$ -V5 and  $\beta_{4b(1-481)}$ -V5 to the same levels as observed in the young neurons. Thus, the full-length  $\beta_{4b}$ -V5 and the truncated  $\beta_{4b(1-481)}$ -V5 subunits do not differ with respect to their nuclear targeting properties in neurons. Both accumulate in the nuclei of young, presumably electrically silent hippocampal neurons, and in differentiated neurons when electrical activity is blocked.

#### Similar nuclear targeting properties of the full-length $\beta_{4b}$ -V5 and the truncated $\beta_{4b(1-481)}$ -V5 subunits in tsA-201 cells

So far our results demonstrate that truncation of the C-terminus of  $\beta_{4b}$  does not interfere with its nuclear targeting properties in muscle and nerve cells. Because previous studies reported a failure of nuclear targeting of  $\beta_{4b(1-481)}$  in CHO and HEK293 cells, we next examined the possibility that this failed nuclear targeting of  $\beta_{4b(1-481)}$  might be particular to non-excitable cells. Therefore we also analyzed the nuclear targeting properties in tsA-201 cells transfected with  $\beta_{4b}$ -V5 and  $\beta_{4b(1-481)}$ -V5 alone and in combination with GFP- $\text{Ca}_v1.2$  and  $\alpha_2\delta$ -1 subunits. As above,  $\beta_{1a}$ -V5 was used as control and all conditions were immunolabeled and analyzed with anti-V5 as well as with specific  $\beta_1$  and  $\beta_4$  antibodies. When the  $\beta$  subunits were expressed alone,  $\beta_{1a}$ -V5 was localized in the cytoplasm but not in the nucleus. In contrast, both  $\beta_{4b}$ -V5 and the truncated  $\beta_{4b(1-481)}$ -V5 accumulated in the nuclei of tsA-201 cells (Fig. 4A). When co-expressed with GFP- $\text{Ca}_v1.2$ , the  $\alpha_1$  and  $\beta$  subunits formed co-aggregates in the cell periphery (Fig. 4B), indicative of expression of the channel complexes in the plasma membrane. In addition, the  $\beta_{4b}$ -V5

subunits, but not  $\beta_{1a}$ -V5 or GFP- $\text{Ca}_v1.2$ , also accumulated in the nuclei. Again, no differences in the membrane and nuclear distribution patterns of  $\beta_{4b}$ -V5 and  $\beta_{4b(1-481)}$ -V5 were observed (Fig. 4B).

Semiquantitative analysis confirmed that a similar fraction of transfected tsA-201 cells showed nuclear targeting of  $\beta_{4b}$ -V5 and  $\beta_{4b(1-481)}$ -V5 (Fig. 4C and D). Whereas no cells were detected where nuclear staining of  $\beta_{1a}$ -V5 was above cytoplasmic staining levels, full-length and truncated  $\beta_{4b}$ -V5 subunits were concentrated in almost all nuclei of tsA-201 when expressed alone. When co-transfected with  $\text{Ca}_v1.2$  and  $\alpha_2\delta$ -1 the fraction of tsA-201 cells with nuclear targeting was reduced to approximately 60% of tsA-201 cells, but again there was no difference between cells transfected with  $\beta_{4b}$ -V5 or  $\beta_{4b(1-481)}$ -V5. In both conditions the prevalence of nuclear staining appeared somewhat lower when labeled with the  $\beta_4$  antibody (Table 1), most likely due to reduced sensitivity of the  $\beta_4$  antibodies compared with anti-V5. In total this analysis demonstrates that  $\beta_{4b}$  subunits are specifically targeted into the nuclei; that this nuclear targeting was independent of co-expression of  $\text{Ca}_v1.2$ ; and that truncation of the C-terminus did not reduce the targeting efficiency of  $\beta_{4b(1-481)}$ -V5.

## Discussion

The premature-termination mutation R482X of the *CACNB4* gene gives rise to a calcium channel  $\beta_4$  protein lacking the 39 C-terminal amino acids. In humans this mutation has been linked with juvenile myoclonic epilepsy.<sup>10</sup> When coexpressed with  $\text{Ca}_v2.1$  in *Xenopus* oocytes the truncated  $\beta_{4b}$  subunit resulted in calcium currents with slightly increased current amplitudes and an accelerated fast time constant of inactivation. This demonstrated that the R482X mutant  $\beta_4$  subunit normally associated with the pore-forming calcium channel  $\text{Ca}_v2.1$ , facilitated its incorporation in the plasma membrane and modulated its

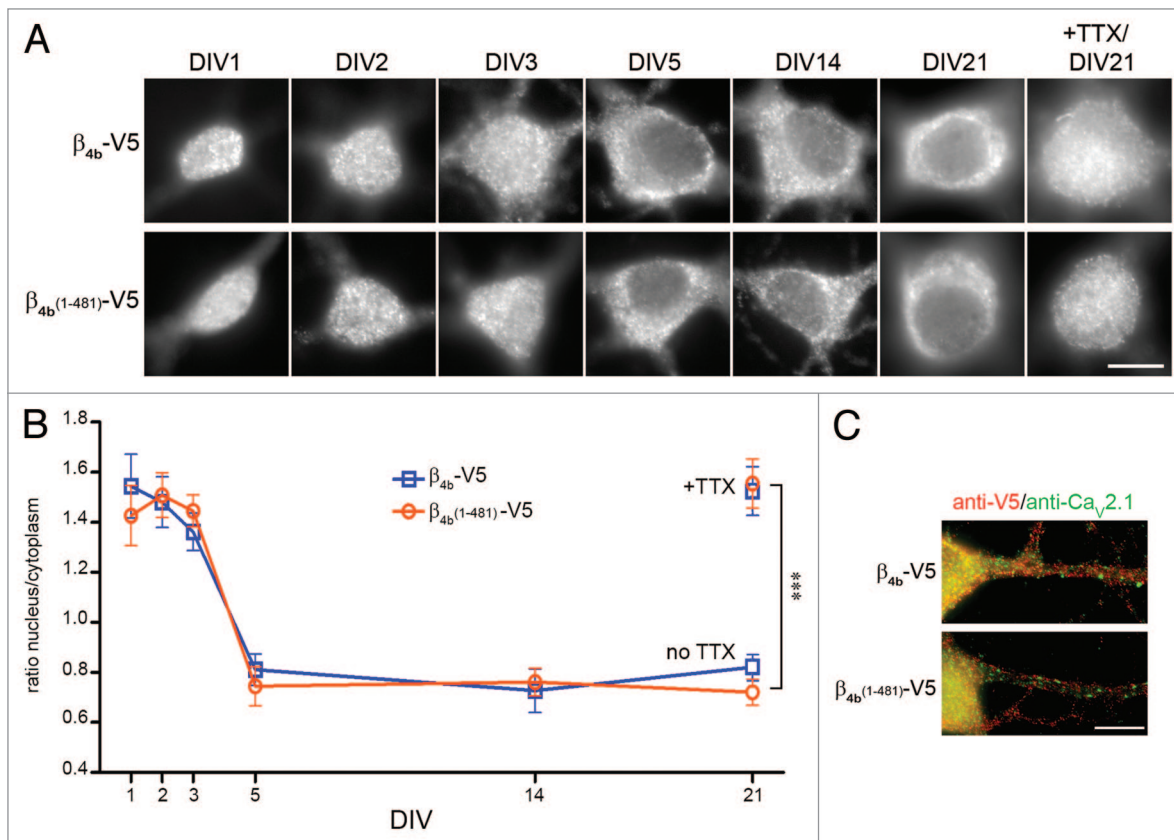


**Figure 3.** Nuclear targeting of full-length  $\beta_{4b}$  and truncated  $\beta_{4b(1-481)}$  subunits in hippocampal neurons differentiating in culture. **(A)** Cultured hippocampal neurons were transfected at DIV 0 (4h after plating) with either  $\beta_{4b}$ -V5 or  $\beta_{4b(1-481)}$ -V5, fixed and immunolabeled with an antibody against the C-terminal V5 epitope at 1, 2, 3, 5, 14 and 21 d in culture (DIV). At DIV21 one set of cultures was treated with  $1\mu\text{M}$  TTX over night to block spontaneous electrical activity. Scale bar,  $10\mu\text{m}$ . **(B)** Nucleus/cytoplasm ratio of cultures shown in **(A)**; including the TTX-treated DIV21 neurons;  $N = 5$ ,  $n = 15-21$  (\*\*\*) =  $P < 0.001$ , unpaired  $t$  test). **(C)** DIV 21 hippocampal neurons double-labeled with anti-V5 and anti- $\text{Ca}_v2.1$  show similar distribution of  $\beta_{4b}$  and  $\beta_{4b(1-481)}$  partially overlapping with synaptic  $\text{Ca}_v2.1$  clusters. Scale bars,  $10\mu\text{m}$ .

gating properties. This interpretation is corroborated by our present findings, where we consistently observed co-clustering of the truncated  $\beta_{4b(1-481)}$  subunits with  $\text{Ca}_v1.1$  and  $\text{Ca}_v1.2$  in skeletal muscle triads and peripheral junctions, co-aggregation of  $\beta_{4b(1-481)}$ -V5 with  $\text{Ca}_v1.2$  in the plasma membrane of tsA-201 cells, and clustering of  $\beta_{4b(1-481)}$ -V5 throughout the axons and dendrites of hippocampal neurons. Thus, despite the truncation of the C-terminus tagged and untagged  $\beta_{4b(1-481)}$  subunits can associate with L-type and non-L-type calcium channels and appears to be normally incorporated into native calcium channel complexes in skeletal muscle cells and neurons.

This raises the question as to whether the modest functional differences between calcium channels containing the wildtype or truncated  $\beta_{4b}$  subunits<sup>10</sup> can be responsible for the neuronal disease phenotype. In fact, lethargic mice—which carry a mutation in the *Cacnb4* gene resulting in the total lack of the  $\beta_4$  proteins—as well as mice with loss-of-function mutations of the primary calcium channel partner of  $\beta_4$  in cerebellum,  $\text{Ca}_v2.1$ , develop similar ataxic and epileptic phenotypes.<sup>9,26-29</sup> These similarities of phenotypes are consistent with a synaptic defect being the primary cause of the ataxia and epilepsy also in  $\beta_{4b}$  mutants. However, a recent study demonstrated that ablation of

$\text{Ca}_v2.1$  function specifically in cerebellar granule cell synapses did not generate ataxia and epilepsy.<sup>30</sup> In comparison to the severe impairment of synaptic function in  $\text{Ca}_v2.1$  knockouts the expected effects from the  $\beta_4\text{R482X}$  mutation would be rather mild. In particular since there may be functional compensation by other  $\beta$  subunit isoforms expressed in the cerebellum.<sup>17,25</sup> Consequently, other, ideally unique properties of  $\beta_4$  subunits may be the primary cause of the neurological phenotype.

One such unique property of the  $\beta_4$  subunit is its ability to accumulate in the cell nucleus.<sup>13-15</sup> Because  $\beta_4$  interacts with nuclear proteins involved in epigenetic regulation of genes,<sup>14,16,18</sup> altered gene regulation might play a role in the etiology of epilepsy in patients with the R482X mutation. Indeed, the ability of  $\beta_4$  to regulate genes in neurons depends on the nuclear targeting properties of its splice variants<sup>17</sup> and heterologous expression of full-length  $\beta_{4b}$  and truncated  $\beta_{4b(1-481)}$  resulted in differential gene regulation in HEK293 cells.<sup>19</sup> Thus, a model has been suggested, according to which  $\beta_{4b}$  forms a complex with B56 $\delta$ /PP2A that is translocated into the nucleus where, in combination with HP1 $\gamma$ , it modifies histone H3 and consequently transcriptional regulation.<sup>16,19</sup> Most importantly for the issue addressed in the present study, Tadmouri et al.<sup>16</sup> asserted that “the formation, as

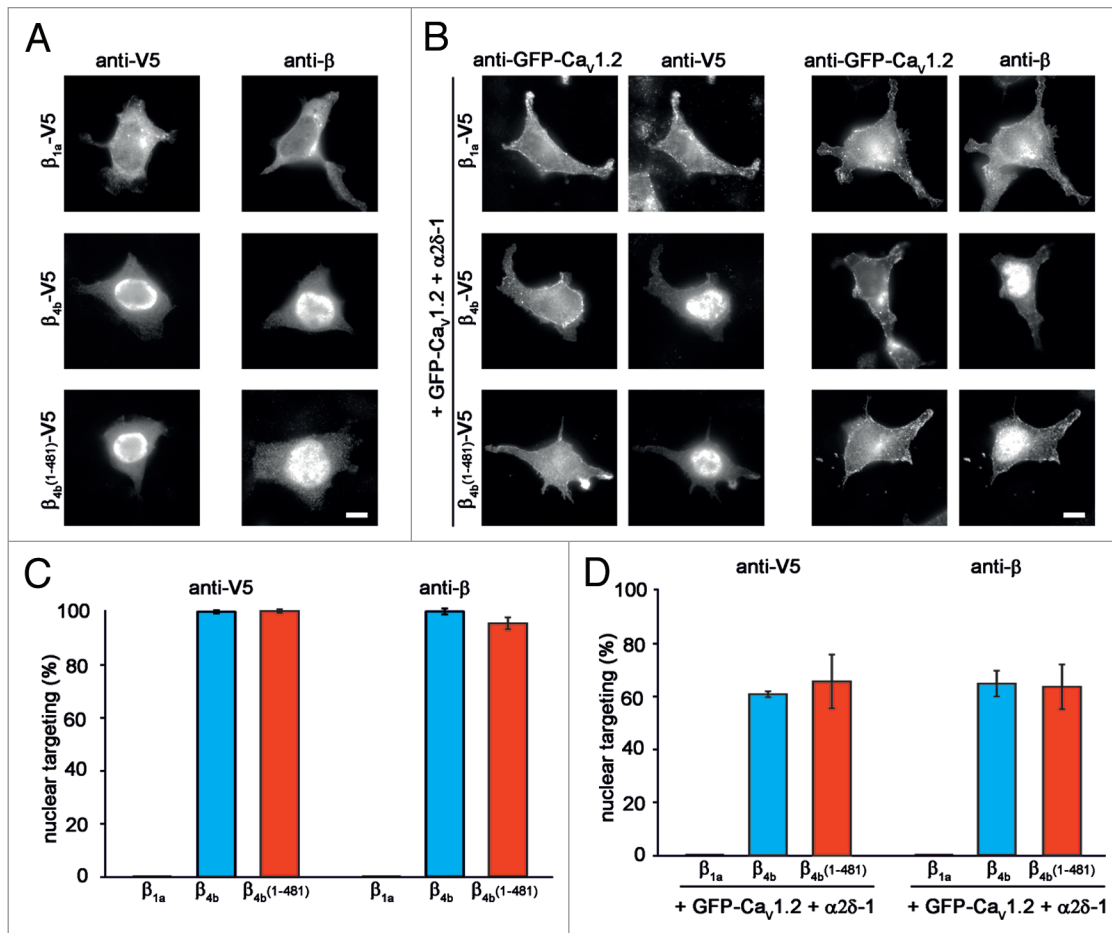


**Figure 4.** Nuclear targeting of full-length  $\beta_{4b}$  and truncated  $\beta_{4b(1-481)}$  subunits in tsA-201 cells. tsA-201 cells were transfected with  $\beta_{1a}$ -V5,  $\beta_{4b}$ -V5 and  $\beta_{4b(1-481)}$ -V5 alone, or in combination with GFP- $\text{Ca}_v1.2/\alpha_2\delta-1$  and immunolabeled with anti-GFP and anti-V5 or anti- $\beta$ . (A) Representative immunofluorescence images of  $\beta$  subunits expressed alone; and (B), of  $\beta$  subunits expressed together with GFP- $\text{Ca}_v1.2/\alpha_2\delta-1$ . (C) Fraction of cells showing nuclear targeting when  $\beta$  subunits were expressed alone (N = 3; anti-V5 n = 180, anti- $\beta$  n = 90); and (D), when  $\beta$  subunits were expressed together with  $\text{Ca}_v1.2/\alpha_2\delta-1$  (N = 3; anti-V5 n = 180, anti- $\beta$  n = 90). Note that the  $\beta$  subunits are cytoplasmic in the absence of an  $\alpha$  subunit, but co-aggregate in the plasma membrane in the presence of  $\text{Ca}_v1.2$ . Nuclear staining is reduced in the presence of  $\text{Ca}_v1.2/\alpha_2\delta-1$ , but still equally abundant with both  $\beta_{4b}$  constructs. Scale bars, 10  $\mu\text{m}$ .

well as the nuclear translocation, of the  $\beta_4$ /B56d/PP2A complex is totally impaired by the premature R482X mutation of  $\beta_4$ .<sup>219</sup>

Our results presented here do not support this notion. In contrast, we examined the nuclear targeting of the truncated  $\beta_{4b(1-481)}$  subunit in three different cell models and found no difference of its nuclear targeting properties compared with full-length  $\beta_{4b}$ . Normal nuclear targeting of  $\beta_{4b(1-481)}$  was observed in differentiated excitable cells (myotubes and hippocampal neurons), in which both  $\beta_{4b}$  constructs were also incorporated in native calcium signaling complexes (triads and synapses). But also when expressed in tsA-201 cells, with and without the  $\text{Ca}_v1.2$   $\alpha_1$  subunit, the truncated  $\beta_{4b(1-481)}$  construct was targeted to the nucleus. Furthermore, in myotubes nuclear targeting of  $\beta_{4b(1-481)}$  was similarly observed with V5-tagged and untagged constructs. This excludes the possibility that the differences between our findings and those of Tadmouri et al.<sup>16</sup> resulted from differences in the used  $\beta_{4b(1-481)}$  constructs or from distinct nuclear targeting mechanisms in different cell types.

Their data indicate the importance for nuclear targeting of C-terminal residues and of intramolecular SH3/GK interactions.<sup>16</sup> In contrast, the equal nuclear targeting of full-length  $\beta_{4b}$  and truncated  $\beta_{4b(1-481)}$  subunits observed here indicates that other variable regions of  $\beta_{4b}$  determine its nuclear targeting properties. Previously we demonstrated the importance of N-terminal residues of  $\beta_{4b}$  for isoform-specific nuclear targeting.<sup>15</sup> This was further corroborated by our recent discovery of a new splice variant ( $\beta_{4c}$ ), which essentially lacks the variable N-terminus and displays no nuclear targeting.<sup>17</sup> The localization of  $\beta_{4b}$  subunits in the nucleus is further regulated by a CRM1-dependent nuclear export mechanism.<sup>15</sup> Consistent with the existence of an activity-dependent  $\beta_{4b}$  nuclear export mechanism, we observed  $\beta_{4b}$  nuclear targeting in young and electrically silent, but not in differentiated hippocampal neurons.<sup>15,17</sup> Moreover we showed that nuclear localization of  $\beta_{4b}$  was lost upon KCl depolarization in myotubes and increased after blocking electrical activity with TTX in myotubes and in hippocampal neurons.<sup>15,17</sup> In the



present study we extended these observations to the truncated  $\beta_{4b(1-481)}$ , which in response to TTX treatment accumulated in the nuclei of differentiated hippocampal neurons as potently as full-length  $\beta_{4b}$ .

Taken together, our present results clearly demonstrate that nuclear targeting and nuclear export properties of  $\beta_{4b}$  and  $\beta_{4b(1-481)}$  are indistinguishable, both in excitable cells and in heterologous expression systems. These findings contest a role of the R482X epilepsy mutation in perturbing nuclear targeting of  $\beta_4$  and they raise serious concerns about the effects of the mutation on gene regulation.<sup>19</sup> Nevertheless, it is important to note that even when nuclear targeting of  $\beta_{4b(1-481)}$  remained intact, this does not exclude the possibility that within the nucleus the interactions of the C-terminally truncated  $\beta_{4b(1-481)}$  with B56 $\gamma$ /PP2A and HP1 $\gamma$  might be perturbed. Whereas this possibility would preclude a model according to which complex formation of  $\beta_4$  and B56 $\gamma$  is a prerequisite for nuclear translocation, it would still be consistent with many of the biochemical data of Tadmouri et al. (2012) as well as with the observation that  $\beta_{4b}$  and  $\beta_{4b(1-481)}$  differentially regulate genes in HEK293 cells.<sup>19</sup>

Clearly the function of the  $\beta_{4b}$  subunit in the nucleus is still far from being understood. Additional experiments will be necessary to resolve the conflicting findings as well as to settle the important problem as to whether the nuclear function of calcium channel  $\beta_4$  subunits is critically involved in the etiology of epilepsy and ataxia in patients and mouse models with mutations in the *CACNB4* gene.

## Materials and Methods

### Expression plasmids

Cloning procedures were previously described for: GFP-Ca $\nu$ 1.1 (NM\_001101720) and GFP-Ca $\nu$ 1.2 (X15539),<sup>31</sup> p $\beta$ A- $\beta$ 1a-V5 (M25514),<sup>24</sup> and p $\beta$ A- $\beta$ 4b-V5 (L02315),<sup>15</sup>  $\alpha_2\delta$ -1 (NM\_001082276),<sup>32</sup> p $\beta$ A- $\beta$ 4b (L02315).<sup>17</sup> To construct p $\beta$ A- $\beta_{4b(1-481)}$ -V5 the p $\beta$ A- $\beta_{4b}$ -V5 (L02315) was used as a template, the deletions of amino acids 482–519 was introduced by SOE-PCR. Briefly, the 3' cDNA sequence coding for the C-terminus of  $\beta_{4b}$  was PCR amplified with overlapping mutagenesis primers in separate PCR reactions using p $\beta$ A- $\beta_{4b}$ -V5 (L02315) as template. Further the two separate PCR products were then used as templates for a final PCR reaction with flanking primers to connect the nucleotide sequences. This fragment was then BglIII/SalI digested and cloned into the respective sites of p $\beta$ A- $\beta_{4b}$ -V5 (L02315) yielding p $\beta$ A- $\beta_{4b(1-481)}$ -V5. To construct p $\beta$ A- $\beta_{4b(1-481)}$ , p $\beta$ A- $\beta_{4b}$ -V5 (L02315) was used as a template and the 3' cDNA sequence coding for the C-terminus of  $\beta_{4b}$  was PCR amplified with a modified reverse primer introducing a stop codon after residue 481. The PCR fragment was then EcoRV/XbaI digested and cloned into the respective sites of p $\beta$ A- $\beta_{4b}$ -V5, yielding p $\beta$ A- $\beta_{4b(1-481)}$ . Note that to be consistent with published literature<sup>10,16,19</sup> we named the truncated  $\beta_{4b}$  construct  $\beta_{4b(1-481)}$ . However in the *Cacnb4* gene (L02315) the R-to-X mutation occurs at amino acid position 481, and not at position 482, as previously described, so the truncated constructs actually end with amino acid 480.

### Myotube cell culture and transfection

Myotubes of the homozygous dysgenic (mdg/mdg) cell line GLT were cultured as previously described.<sup>33</sup> At the onset of myoblast fusion, GLT cell cultures were transfected with plasmids coding for the calcium channel subunits using FuGeneHD transfection reagent (Promega) according to the manufacturer's instructions. A total of 1  $\mu$ g of plasmid DNA was used per 30 mm culture dish.

### Hippocampal cultures

Low-density cultures of hippocampal neurons were prepared from 17 d-old embryonic BALB/c mice of either sex as described previously.<sup>34-36</sup> Neurons were plated on poly-L-lysine-coated glass coverslips in 60-mm culture dishes at a density of ~3500 cells/cm<sup>2</sup>. After plating, cells were allowed to attach for 3–4 h before transferring the coverslips neuron-side-down into a 60-mm culture dish with a glial feeder layer. For maintenance, the neurons and glial feeder layer were cultured in serum-free neurobasal medium (Invitrogen) supplemented with Glutamax and B27 supplements (Invitrogen). Ara-C (5  $\mu$ M) was added 3 d after plating and once a week 1/3 of medium was removed and replaced with fresh maintenance medium.

### Transfection of hippocampal neurons

Cultured hippocampal neurons were transfected with p $\beta$ A- $\beta_{4b}$ -V5 and p $\beta$ A- $\beta_{4b(1-481)}$ -V5 constructs immediately after plating for 4 h using Lipofectamine 2000-mediated transfection reagent (Invitrogen) as previously described<sup>36</sup> a total amount of 0.05  $\mu$ g DNA was used per each condition. Transfected neurons were used for experiments from DIV 1 onwards.

### tsA-201 cell culture and transfection

tsA-201 cells were cultured in Dulbecco's modified Eagle's medium (DMEM) supplemented with 0.44 M NaHCO<sub>3</sub>, 10% fetal calf serum (Gibco, 500–064), 2 mM glutamine (Sigma, G753) penicillin (10 units/ml) and streptomycin (10  $\mu$ g/ml) and maintained at 37 °C in a humidified environment with 5% CO<sub>2</sub>. Cells were grown and transiently transfected when they reached about 80% of confluency with FuGeneHD transfection reagent (Roche Diagnostics) according to the manufacturer's instructions. A total of 0.25  $\mu$ g of plasmid DNA was used per 30 mm culture dish. Cells were replated 24 h after transfection onto 13 mm poly-L-lysine coated coverslips and kept at 30 °C, 5% CO<sub>2</sub> for 24 h prior to fixation.

### Immunocytochemistry and microscopy

Cells were immunostained as described in<sup>37</sup> for myotubes and in<sup>36</sup> for neurons. Briefly, cells were fixed in 4% paraformaldehyde/4% sucrose in PBS (pF) at room temperature for 20 min and incubated in 5% normal goat serum in PBS containing 0.2% bovine serum albumin (BSA) and 0.2% Triton X-100 (PBS/BSA/Triton) for 30 min. Primary antibodies; mouse monoclonal anti- $\beta_1$  (1:2000) and anti- $\beta_4$  (1:500) (both NeuroMab, UC Davis/NIH NeuroMab Facility), mouse monoclonal anti-V5 (1:400; Invitrogen), polyclonal anti-GFP (1:10000; Molecular Probes, Eugene, OR, USA) were applied in PBS/BSA/Triton for 4 h at RT, washed in PBS and then stained with goat anti-rabbit Alexa 488 and/or goat anti-mouse Alexa 594 (1:4000, Molecular Probes) for 1 h at RT. After staining coverslips were washed and mounted in Vectashield to avoid photo bleaching. Preparations were analyzed on an AxioImager microscope (Carl Zeiss, Inc.,) using a 63x 1.4 NA



objective. 14-bit images were recorded with a cooled CCD camera (SPOT or INSIGHT; Diagnostic Instruments, Stirling Heights, MI, USA) and Metaview image processing software (Universal Imaging, Corp., West Chester, PA, USA). Figures were arranged in Adobe Photoshop CS6 (Adobe Systems Inc.,) and where necessary contrast, black level and gamma were adjusted to optimally display the labeling patterns.

#### Nuclear targeting analysis in myotubes and tsA-201 cells

Cultures labeled with anti-GFP and anti-V5 or anti- $\beta$  were systematically screened for transfected, well differentiated myotubes or tsA-201 cells based on the GFP-Ca<sub>v</sub>1 staining (green channel) and nuclear staining of the  $\beta$  subunits was analyzed after switching to the red filter channel.<sup>15</sup> Nuclear targeting was rated positive, when the fluorescence intensity of any nuclei in the myotube was above that of the cytoplasm. The degree of nuclear targeting in dysgenic myotubes was determined by calculating the nucleus/cytoplasm ratio of the anti-V5 fluorescence intensity, after background subtraction using *Metamorph* software. Results are expressed as mean  $\pm$  SEM. All data were organized in *MS Excel* and analyzed using ANOVA with Tukey post-hoc analysis in *Excel* with *Daniel's XL* toolbox.

#### Nuclear targeting analysis in neurons

The degree of nuclear targeting in cultured hippocampal neurons was determined by calculating the nucleus/cytoplasm ratio of the anti- $\beta_4$  fluorescence intensity, the analysis was performed by a semi-automated procedure using a custom programmed *Metamorph Macro* journal as described in.<sup>17</sup>

#### Statistical analysis

Results are expressed as means  $\pm$  SEM except where otherwise indicated. "N" indicates the number of independent experiments and "n" the total number of analyzed cells. Data were organized and analyzed in *Excel* and *GraphPad*.

#### References

- Buraei Z, Yang J. The  $\beta$  subunit of voltage-gated Ca<sup>2+</sup> channels. *Physiol Rev* 2010; 90:1461-506; PMID:20959621; <http://dx.doi.org/10.1152/physrev.00057.2009>
- Ball SL, Gregg RG. Using mutant mice to study the role of voltage-gated calcium channels in the retina. *Adv Exp Med Biol* 2002; 514:439-50; PMID:12596937; [http://dx.doi.org/10.1007/978-1-4615-0121-3\\_26](http://dx.doi.org/10.1007/978-1-4615-0121-3_26)
- Gregg RG, Messing A, Strube C, Beurq M, Moss R, Behan M, Sukhareva M, Haynes S, Powell JA, Coronado R, et al. Absence of the beta subunit (cchb1) of the skeletal muscle dihydropyridine receptor alters expression of the alpha 1 subunit and eliminates excitation-contraction coupling. *Proc Natl Acad Sci U S A* 1996; 93:13961-6; PMID:8943043; <http://dx.doi.org/10.1073/pnas.93.24.13961>
- Neef J, Gehrt A, Bulankina AV, Meyer AC, Riedel D, Gregg RG, Strenzke N, Moser T. The Ca<sup>2+</sup> channel subunit beta2 regulates Ca<sup>2+</sup> channel abundance and function in inner hair cells and is required for hearing. *J Neurosci* 2009; 29:10730-40; PMID:19710324; <http://dx.doi.org/10.1523/JNEUROSCI.1577-09.2009>
- Weisserger P, Held B, Bloch W, Kaestner L, Chien KR, Fleischmann BK, Lipp P, Flockerzi V, Freichel M. Reduced cardiac L-type Ca<sup>2+</sup> current in Ca(V)beta2<sup>-/-</sup> embryos impairs cardiac development and contraction with secondary defects in vascular maturation. *Circ Res* 2006; 99:749-57; PMID:16946137; <http://dx.doi.org/10.1161/01.RES.0000243978.15182.c1>
- Jeon D, Song I, Guido W, Kim K, Kim E, Oh U, Shin HS. Ablation of Ca<sup>2+</sup> channel beta3 subunit leads to enhanced N-methyl-D-aspartate receptor-dependent long term potentiation and improved long term memory. *J Biol Chem* 2008; 283:12093-101; PMID:18339621; <http://dx.doi.org/10.1074/jbc.M800816200>
- Murakami M, Nakagawasa O, Yanai K, Nunoki K, Tan-No K, Tadano T, Iijima T. Modified behavioral characteristics following ablation of the voltage-dependent calcium channel beta3 subunit. *Brain Res* 2007; 1160:102-12; PMID:17588550; <http://dx.doi.org/10.1016/j.brainres.2007.05.041>
- Obermair G, Flucher B. Neuronal Functions of Auxiliary Calcium Channel Subunits. In: Stephens G, Mochida S, eds. *Modulation of Presynaptic Calcium Channels*; Springer Netherlands, 2013:29-59.
- Burgess DL, Jones JM, Meisler MH, Noebels JL. Mutation of the Ca<sup>2+</sup> channel beta subunit gene *Cchb4* is associated with ataxia and seizures in the lethargic (lh) mouse. *Cell* 1997; 88:385-92; PMID:9039265; [http://dx.doi.org/10.1016/S0092-8674\(00\)81877-2](http://dx.doi.org/10.1016/S0092-8674(00)81877-2)
- Escayg A, De Waard M, Lee DD, Bichet D, Wolf P, Mayer T, Johnston J, Baloh R, Sander T, Meisler MH. Coding and noncoding variation of the human calcium-channel beta4-subunit gene *CACNB4* in patients with idiopathic generalized epilepsy and episodic ataxia. *Am J Hum Genet* 2000; 66:1531-9; PMID:10762541; <http://dx.doi.org/10.1086/302909>
- Barclay J, Balaguero N, Mione M, Ackerman SL, Letts VA, Brodbeck J, Canti C, Meir A, Page KM, Kusumi K, et al. Ducky mouse phenotype of epilepsy and ataxia is associated with mutations in the *Cacna2d2* gene and decreased calcium channel current in cerebellar Purkinje cells. *J Neurosci* 2001; 21:6095-104; PMID:11487633
- Fletcher CF, Lutz CM, O'Sullivan TN, Shaughnessy JD Jr, Hawkes R, Frankel WN, Copeland NG, Jenkins NA. Absence epilepsy in tottering mutant mice is associated with calcium channel defects. *Cell* 1996; 87:607-17; PMID:8929530; [http://dx.doi.org/10.1016/S0092-8674\(00\)81381-1](http://dx.doi.org/10.1016/S0092-8674(00)81381-1)
- Colecraft HM, Alseikhan B, Takahashi SX, Chaudhuri D, Mittman S, Yegnasubramanian V, Alvania RS, Johns DC, Marbán E, Yue DT. Novel functional properties of Ca(2+) channel beta subunits revealed by their expression in adult rat heart cells. *J Physiol* 2002; 541:435-52; PMID:12042350; <http://dx.doi.org/10.1113/jphysiol.2002.018515>
- Hibino H, Pironkova R, Onwumere O, Rousset M, Charner P, Hudspeth AJ, Lesage F. Direct interaction with a nuclear protein and regulation of gene silencing by a variant of the Ca<sup>2+</sup>-channel beta 4 subunit. *Proc Natl Acad Sci U S A* 2003; 100:307-12; PMID:12518067; <http://dx.doi.org/10.1073/pnas.0136791100>

#### Western blot

DIV 7 GLTs expressing p $\beta$ A- $\beta_{4b}$ -V5 or p $\beta$ A- $\beta_{4b(1-481)}$ -V5 were trypsinized, centrifuged, resuspended and lysed in RIPA buffer (50 mM TRIS-HCl, pH 8; 150 mM NaCl<sub>2</sub>; 10 mM NaF; 0.5 mM EDTA; 0.10% SDS; 10% glycerol; 1% igepal; 1x Protease Inhibitor Complete cocktail (Roche)) with a pestle and left on ice for 30 min. The lysates were then purified by centrifugation (4000 g, 10 min, 4 °C). Protein concentrations were determined using a BCA assay (Thermo Scientific) according to manufacturer's instructions. Thirty micrograms of protein were separated by SDS-PAGE (10%) at 196 V and 40 mA for 60 min and transferred to a PVDF membrane at 25 V and 100 mA for 3 h at 4 °C with a semidry-blotting system (Roth). The blot was incubated with mouse anti-V5 (1:5000; Invitrogen) or mouse anti- $\beta_4$  (1:10,000; Neuromab) antibodies overnight at 4 °C and successively with HRP-conjugated secondary antibody (1:5000; Pierce) for 1 h at room temperature. The chemiluminescent signal was detected with ECL Supersignal West Pico kit (Thermo Scientific) and visualized with ImageQuant LAS 4000.

#### Disclosure of Potential Conflicts of Interest

No potential conflicts of interest were disclosed.

#### Acknowledgments

We thank Ariane Benedetti for excellent assistance with molecular biology, providing the muscle cultures and performing the western blots, Ruslan Stanika for providing hippocampal neurons, and Alexandra Pinggera for providing transfected tsA-201 cells. This work was supported by research grants from the Austrian Science Fund (FWF) P23479, F04406 and W1101.

15. Subramanyam P, Obermair GJ, Baumgartner S, Gebhart M, Striessnig J, Kaufmann WA, Geley S, Flucher BE. Activity and calcium regulate nuclear targeting of the calcium channel beta4b subunit in nerve and muscle cells. *Channels (Austin)* 2009; 3:343-55; PMID:19755859; <http://dx.doi.org/10.4161/chan.3.5.9696>
16. Tadmouri A, Kiyonaka S, Barbado M, Rousset M, Fablet K, Sawamura S, Bahembera E, Pernet-Gallay K, Arnoult C, Miki T, et al. Cacnb4 directly couples electrical activity to gene expression, a process defective in juvenile epilepsy. *EMBO J* 2012; 31:3730-44; PMID:22892567; <http://dx.doi.org/10.1038/emboj.2012.226>
17. Etemad S, Obermair GJ, Bindreither D, Benedetti A, Stanika R, Di Biase V, Burtcher V, Koschak A, Kofler R, Geley S, et al. Differential neuronal targeting of a new and two known calcium channel beta4 subunit splice variants correlates with their regulation of gene expression. *J Neurosci* 2014; 34:1446-61; PMID:24453333; <http://dx.doi.org/10.1523/JNEUROSCI.3935-13.2014>
18. Xu X, Lee YJ, Holm JB, Terry MD, Oswald RE, Horne WA. The Ca2+ channel beta4c subunit interacts with heterochromatin protein 1 via a PXVXL binding motif. *J Biol Chem* 2011; 286:9677-87; PMID:21220418; <http://dx.doi.org/10.1074/jbc.M110.187864>
19. Ronjat M, Kiyonaka S, Barbado M, De Waard M, Mori Y. Nuclear life of the voltage-gated Cacnb4 subunit and its role in gene transcription regulation. *Channels (Austin)* 2013; 7:119-25; PMID:23511121; <http://dx.doi.org/10.4161/chan.23895>
20. Neuhuber B, Gerster U, Döring F, Glossmann H, Tanabe T, Flucher BE. Association of calcium channel alpha1S and beta1a subunits is required for the targeting of beta1a but not of alpha1S into skeletal muscle triads. *Proc Natl Acad Sci U S A* 1998; 95:5015-20; PMID:9560220; <http://dx.doi.org/10.1073/pnas.95.9.5015>
21. Campiglio M, Di Biase V, Tuluc P, Flucher BE. Stable incorporation versus dynamic exchange of beta subunits in a native Ca2+ channel complex. *J Cell Sci* 2013; 126:2092-101; PMID:23447673; <http://dx.doi.org/10.1242/jcs.jcs124537>
22. Kasielke N, Obermair GJ, Kugler G, Grabner M, Flucher BE. Cardiac-type EC-coupling in dysgenic myotubes restored with Ca2+ channel subunit isoforms alpha1C and alpha1D does not correlate with current density. *Biophys J* 2003; 84:3816-28; PMID:12770887; [http://dx.doi.org/10.1016/S0006-3495\(03\)75109-1](http://dx.doi.org/10.1016/S0006-3495(03)75109-1)
23. Tuluc P, Kern G, Obermair GJ, Flucher BE. Computer modeling of siRNA knockdown effects indicates an essential role of the Ca2+ channel alpha2delta-1 subunit in cardiac excitation-contraction coupling. *Proc Natl Acad Sci U S A* 2007; 104:11091-6; PMID:17563358; <http://dx.doi.org/10.1073/pnas.0700577104>
24. Obermair GJ, Schlick B, Di Biase V, Subramanyam P, Gebhart M, Baumgartner S, Flucher BE. Reciprocal interactions regulate targeting of calcium channel beta subunits and membrane expression of alpha1 subunits in cultured hippocampal neurons. *J Biol Chem* 2010; 285:5776-91; PMID:19996312; <http://dx.doi.org/10.1074/jbc.M109.044271>
25. Schlick B, Flucher BE, Obermair GJ. Voltage-activated calcium channel expression profiles in mouse brain and cultured hippocampal neurons. *Neuroscience* 2010; 167:786-98; PMID:20188150; <http://dx.doi.org/10.1016/j.neuroscience.2010.02.037>
26. Kodama T, Itsukaichi-Nishida Y, Fukazawa Y, Wakamori M, Miyata M, Molnar E, Mori Y, Shigemoto R, Imoto K. A CaV2.1 calcium channel mutation rocker reduces the number of postsynaptic AMPA receptors in parallel fiber-Purkinje cell synapses. *Eur J Neurosci* 2006; 24:2993-3007; PMID:17156361; <http://dx.doi.org/10.1111/j.1460-9568.2006.05191.x>
27. Lonchamp E, Dupont JL, Doussau F, Shin HS, Poulain B, Bossu JL. Deletion of Cav2.1 (alpha1(A)) subunit of Ca2+-channels impairs synaptic GABA and glutamate release in the mouse cerebellar cortex in cultured slices. *Eur J Neurosci* 2009; 30:2293-307; PMID:20092572; <http://dx.doi.org/10.1111/j.1460-9568.2009.07023.x>
28. Matsushita K, Wakamori M, Rhyu IJ, Arii T, Oda S, Mori Y, Imoto K. Bidirectional alterations in cerebellar synaptic transmission of tottering and rolling Ca2+ channel mutant mice. *J Neurosci* 2002; 22:4388-98; PMID:12040045
29. Walter JT, Alviña K, Womack MD, Chevez C, Khodakhah K. Decreases in the precision of Purkinje cell pacemaking cause cerebellar dysfunction and ataxia. *Nat Neurosci* 2006; 9:389-97; PMID:16474392; <http://dx.doi.org/10.1038/nn1648>
30. Galliano E, Gao Z, Schonewille M, Todorov B, Simons E, Pop AS, D'Angelo E, van den Maagdenberg AM, Hoebeek FE, De Zeeuw CI. Silencing the majority of cerebellar granule cells uncovers their essential role in motor learning and consolidation. *Cell Rep* 2013; 3:1239-51; PMID:23583179; <http://dx.doi.org/10.1016/j.celrep.2013.03.023>
31. Grabner M, Dirksen RT, Beam KG. Tagging with green fluorescent protein reveals a distinct subcellular distribution of L-type and non-L-type Ca2+ channels expressed in dysgenic myotubes. *Proc Natl Acad Sci U S A* 1998; 95:1903-8; PMID:9465115; <http://dx.doi.org/10.1073/pnas.95.4.1903>
32. Bock G, Gebhart M, Scharinger A, Jangsanthong W, Busquet P, Poggiani C, Sartori S, Mangoni ME, Sinnegger-Brauns MJ, Herzig S, et al. Functional properties of a newly identified C-terminal splice variant of Cav1.3 L-type Ca2+ channels. *J Biol Chem* 2011; 286:42736-48; PMID:21998310; <http://dx.doi.org/10.1074/jbc.M111.269951>
33. Powell JA, Petherbridge L, Flucher BE. Formation of triads without the dihydropyridine receptor alpha subunits in cell lines from dysgenic skeletal muscle. *J Cell Biol* 1996; 134:375-87; PMID:8707823; <http://dx.doi.org/10.1083/jcb.134.2.375>
34. Kaech S, Banker G. Culturing hippocampal neurons. *Nat Protoc* 2006; 1:2406-15; PMID:17406484; <http://dx.doi.org/10.1038/nprot.2006.356>
35. Obermair GJ, Kaufmann WA, Knaus HG, Flucher BE. The small conductance Ca2+-activated K+ channel SK3 is localized in nerve terminals of excitatory synapses of cultured mouse hippocampal neurons. *Eur J Neurosci* 2003; 17:721-31; PMID:12603262; <http://dx.doi.org/10.1046/j.1460-9568.2003.02488.x>
36. Obermair GJ, Szabo Z, Bourinet E, Flucher BE. Differential targeting of the L-type Ca2+ channel alpha 1C (CaV1.2) to synaptic and extrasynaptic compartments in hippocampal neurons. *Eur J Neurosci* 2004; 19:2109-22; PMID:15090038; <http://dx.doi.org/10.1111/j.0953-816X.2004.03272.x>
37. Flucher BE, Weiss RG, Grabner M. Cooperation of two-domain Ca(2+) channel fragments in triad targeting and restoration of excitation-contraction coupling in skeletal muscle. *Proc Natl Acad Sci U S A* 2002; 99:10167-72; PMID:12119388; <http://dx.doi.org/10.1073/pnas.122345799>